Random walk model for dual cascades in wave turbulence

Oliver Bühler*
Courant Institute of Mathematical Sciences, New York University, New York, New York 10012, USA

(Received 4 November 2023; revised 14 March 2024; accepted 5 April 2024; published 1 May 2024)

Dual cascades in turbulent systems with two conserved quadratic quantities famously arise in both two-dimensional hydrodynamic turbulence and also in wave turbulence based on four-wave interactions. Examples for the latter include surface waves and nonlinear Schrödinger equations with cubic nonlinearity. However, numerical simulations in forced–dissipative equilibrium of two-dimensional turbulence and of a one-dimensional wave system reveal that the physical nature of their cascades is starkly different. This is demonstrated by comparing their spectra in a finite inertial range and by comparing the temporal fluctuations of their spectral fluxes. In particular, the flux fluctuations are much larger in the wave case and frequently lead to instantaneous flux values that have the opposite sign of the mean flux, a phenomenon that is completely absent in the hydrodynamic case. A simple random walk model for the dual cascade in wave turbulence is then formulated that is very successful in explaining these effects. In particular, the model is able to replicate the detailed shape of the observed turbulent spectrum in a finite inertial range, and it also offers a ready explanation for the large flux fluctuations. It is also shown that a nonlinear diffusion model for the wave system cannot explain the observed spectral shapes. Overall, this suggests that in wave turbulence the systematic spectral fluxes observed in a dual cascade do not require an irreversible dynamical mechanism, rather, they arise as the inevitable outcome of blind chance.

DOI: 10.1103/PhysRevE.109.055102

I. INTRODUCTION

The elementary notions of turbulent cascades in hydrodynamic and wave turbulence are discussed, with a focus on dual cascades in forced–dissipative equilibrium. These cascades have the remarkable property that exact turbulent fluxes and flux directions in spectral space can be computed *a priori*, i.e., based only on knowledge of the forcing and dissipation wave numbers.

A. Hydrodynamic turbulence cascades

Spectral energy cascades and inertial ranges are key concepts in hydrodynamic turbulence, going back to the foundational work by Kolmogorov in the 1940s on homogeneous isotropic turbulence [e.g., 1,2]. For example, in three-dimensional incompressible fluid dynamics, the kinetic energy $\mathcal{E} \geqslant 0$ is conserved by smooth solutions of the Euler equations, and because $\mathcal{E}$ is quadratic in the velocity field there is a well-defined spectral energy density $E(k,t) \geqslant 0$ such that

$$\mathcal{E} = \int_0^\infty E \, \mathrm{d}k = \text{const.} \tag{1}$$

Here $k \geqslant 0$ is the wave-number magnitude of the Fourier components. A forced–dissipative stationary state can be reached if energy is continually injected at some forcing wave number k_f and also continually extracted at some larger dissipation wave number k_+ (e.g., by the usual Navier–Stokes dissipation terms, but other dissipation choices exist in numerical practice). Then $E(k,t)$ can be replaced by a time-averaged density $E(k)$, and the spectral energy budget acquires source and sink terms at k_f and k_+, respectively. If the forcing scale is much larger than the dissipation scale, then there is an inertial range of wave numbers k such that

$$k_f \ll k \ll k_+. \tag{2}$$

A constant spectral flux of energy through the inertial range from k_f down to $k_+ \gg k_f$ is then possible. In particular, if P is the energy (per unit time and space) injected at k_f and P_+ is the energy extracted at k_+ then $P = P_+$. (Here P has units of length squared divided by time cubed.) The physical mechanism behind this downscale (or "forward" or "direct") cascade is three-dimensional vortex stretching. Assuming that E in the inertial range depends only on k and P then produces the famous Kolmogorov spectrum $E = CP^{2/3}k^{-5/3}$ from either dimensional analysis or, equivalently, from assuming that the spectrum is self-similar under the scaling symmetries of the Euler equations.

The situation is completely different for two-dimensional incompressible flows [1,2], for which the curl of the velocity field has only a single nonzero component q, which is then materially advected by the flow. Physically this means vortex stretching is absent. The material invariance of q along particle trajectories then implies the trivial integral conservation of all smooth functions $F(q)$. This is because the two-dimensional flow is an area-preserving map that advects the level sets of q and therefore equally the level sets of any $F(q)$. Of primary importance in turbulence theory is the quadratic choice $F(q) = q^2/2$, which leads to the integral conservation of the so-called enstrophy $\mathcal{Z} \geqslant 0$. This is because, like energy,

*obuhler@cims.nyu.edu

enstrophy is also sign-definite and quadratic in the velocity fields, and therefore it, too, has a well-defined spectral density $Z(k,t) \geqslant 0$. Moreover, $Z = k^2 E$ follows from the definition of the curl q and therefore

$$\mathcal{Z} = \int_0^\infty Z \, \mathrm{d}k = \int_0^\infty k^2 E \, \mathrm{d}k = \text{const.} \tag{3}$$

The importance of (3) is that it provides a *second* integral conservation law for E, which is a significant constraint on its evolution. For example, this second constraint makes it clear that the three-dimensional forced–dissipative inertial range scenario is not possible in two-dimensional turbulence. This is because injection at k_f of energy at rate P now also implies injection of enstrophy at rate $k_f^2 P$. Dissipating energy at k_+ with $P_+ = P$ then implies enstrophy dissipation at a rate $k_+^2 P \gg k_f^2 P$, so no stationary state is possible because the enstrophy budget is not closed.

This led to the realization that for stationary two-dimensional turbulence it is necessary to have dissipation both at large wave numbers $k_+ \gg k_f$ and also at small wave numbers $k_- \ll k_f$. This is the scenario of a dual cascade: a forward cascade from k_f to k_+ and an inverse cascade from k_f to k_-. Energy and enstrophy participate with nonequal rates in these cascades and these rates can be computed exactly, a remarkable fact that was first pointed out by Fjørtoft ([3] hereafter F53). This follows from the twin budget constraints

$$P = P_- + P_+ \quad \text{and} \quad k_f^2 P = k_-^2 P_- + k_+^2 P_+. \tag{4}$$

In particular, the proportion of energy dissipated at the low wave number k_- is

$$\frac{P_-}{P} = \frac{k_+^2 - k_f^2}{k_+^2 - k_-^2}, \tag{5}$$

which tends to unity in the ideal limit of an infinitely wide direct inertial range $k_+ \to \infty$. Hence energy goes predominantly upscale in two-dimensional turbulence while the opposite is true for enstrophy, which goes predominantly downscale. Physically, in free evolution this corresponds to the formation and merging of large-scale vortices that contain most of the energy, while most of the enstrophy resides in small-scale filamentary vorticity structures, which are advected and elongated further by the vortices in a nearly passive way. In summary, two-dimensional and three-dimensional hydrodynamic turbulent cascades function very differently, but in both cases there are clear physical mechanisms related to vorticity dynamics that explain these differences and thereby lend robustness to the inertial range theories.

B. Wave turbulence cascades

In wave turbulence flow amplitudes are low by assumption and the dynamics is dominated by dispersive wave modes that evolve slowly in amplitude due to weak interactions with other wave modes [e.g., Refs. 4–7]. Such interactions are strongest when the participating wave modes form nonlinear products whose time dependence projects onto other linear wave frequencies in a resonant or nearly resonant fashion. The dispersion relation and the form of the nonlinear terms dictates the minimum size of interacting wave modes (triads, quartets, etc.) that can form such a resonant group. For deep-water surface waves (and also for the nonlinear Schrödinger equation with cubic nonlinearity) the smallest resonant group is a quartet of four wave modes that satisfy the conditions

$$\mathbf{k}_1 + \mathbf{k}_2 = \mathbf{k}_3 + \mathbf{k}_4 \quad \text{and} \quad \omega_1 + \omega_2 = \omega_3 + \omega_4, \tag{6}$$

where the frequencies $\omega_i = \omega(\mathbf{k}_i) \geqslant 0$ satisfy the linear dispersion relation. [Other sign choices in (6) are relevant to capture all interactions in systems with multiple frequency branches, but this is not important here.] Wave turbulence theory then builds a statistical closure for these interacting quartets, which leads to a kinetic integral equation for the evolution of the mean spectral wave energy density. From hereon we will assume that $\omega(\mathbf{k})$ is isotropic and therefore depends only on $k = |\mathbf{k}|$ and also that $\omega(k)$ is increasing with k.

Conservation laws are as important in wave turbulence as they are in hydrodynamic turbulence. Each resonant quartet (6) conserves the total wave energy, i.e., if E_i is the wave energy in mode i then

$$E_1 + E_2 + E_3 + E_4 = \text{const.} \tag{7}$$

This therefore implies conservation of total wave energy. But each resonant quartet also conserves the so-called wave action per mode, which is $N_i = E_i/\omega_i$. Combining this with (7), we obtain the twin conservation laws for total action and energy as

$$\sum_i N_i = \text{const.} \quad \text{and} \quad \sum_i \omega_i N_i = \text{const.}, \tag{8}$$

where the sum extends over all wave modes in the system. There is now an obvious formal analogy with the twin two-dimensional conservation laws (1) and (3) via

$$(E, Z, k^2) \leftrightarrow (N, E, \omega). \tag{9}$$

This implies a dual cascade in wave turbulence and that a version of F53's rule (5) holds for wave turbulence. Specifically, if the waves are forced at ω_f and dissipated at both $\omega_- < \omega_f$ and $\omega_+ > \omega_f$, then

$$\frac{Q_-}{Q} = \frac{\omega_+ - \omega_f}{\omega_+ - \omega_-} \tag{10}$$

holds for the total action input rate Q and its low-frequency dissipation rate Q_-. Hence wave action flows predominantly upscale and wave energy flows predominantly downscale. This is a convincing mathematical fact, but no ready physical mechanism comes to mind that explains it.

Indeed, the similarity of (10) and (5) may mask significant differences in the nature of the dual cascades in two-dimensional hydrodynamic turbulence and those in wave turbulence. For one thing, wave turbulence is similar to two-dimensional turbulence because of the dual cascades, but it is also similar to three-dimensional turbulence because wave energy goes downscale, not upscale. Another point is that the conservation of hydrodynamic enstrophy is exact whereas the conservation of wave action is sometimes fragile and restricted to resonant wave interactions and the kinetic equation, i.e., it does not hold for the full nonlinear dynamics. For example, this occurs in the case of deep-water surface waves. But arguably most important is the lack of a compelling dynamical

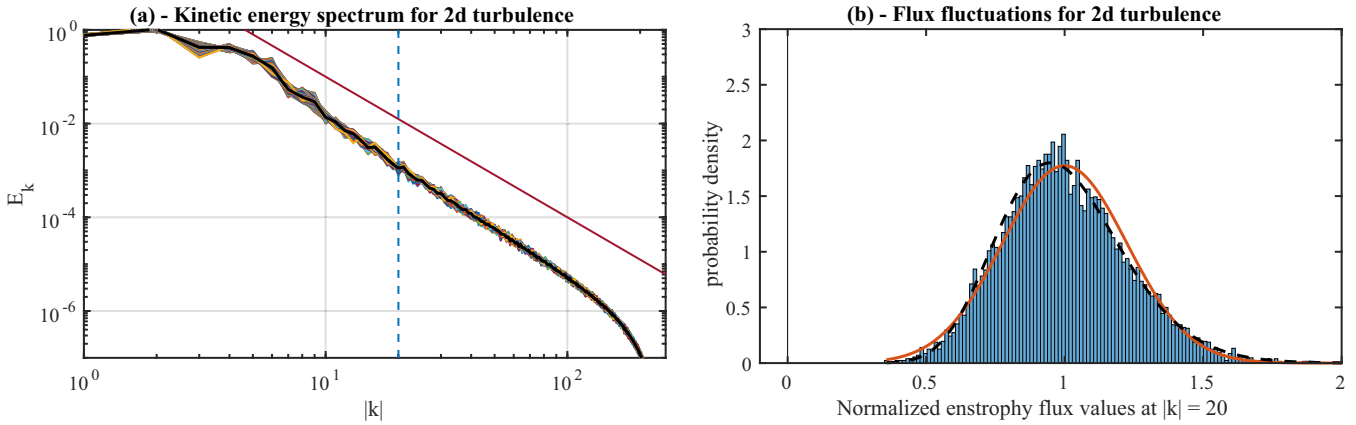

FIG. 1. Left: Energy spectrum in forced–dissipative two-dimensional hydrodynamic turbulence. The flow is forced at $k_f = 5$, and the separate line is the theoretical enstrophy cascade spectrum with slope -3. Right: Histogram of enstrophy flux values (normalized to have unit mean) collected at $k = 20$ (dashed line on the left panel). The standard deviation is 20% of the mean flux, all observed values are positive, there is a poor fit with a normal distribution (solid line), and a better fit with a γ distribution (dashed line).

process that explains the wave cascades physically, in contrast to the well-understood advective dynamics of vorticity in both three-dimensional and two-dimensional hydrodynamic turbulence.

II. NUMERICAL SIMULATION OF DUAL CASCADES

We compare forced–dissipative dual cascades in two-dimensional hydrodynamic turbulence against those in a one-dimensional wave turbulence model. In both cases the focus is on the forward cascade, which in the first case involves enstrophy and in the second case wave energy. Of course, even though we restrict numerical attention to the forward cascade, it is the underlying existence of twin conservation laws and therefore of dual cascades that is absolutely essential.

The hydrodynamic simulation was performed using a standard pseudospectral model with 512×512 Fourier modes. The flow was forced isotropically at wave numbers with magnitude $k_f = 5$ and run to a stationary state. The corresponding mean energy spectrum is shown as the black line in the left panel of Fig. 1. The other lines are snapshots of the instantaneous energy spectrum, which are all close to the mean spectrum. Also indicated by the separate line is the ideal theoretical spectrum $E(k) \propto k^{-3}$ for the forward cascade, which holds well throughout most of the inertial range. In other words, the impact of the dissipation range onto the spectral shape in the inertial range is weak.

The right panel shows a histogram of 10 000 instantaneous enstrophy flux values measured at wave number $k = 20$, which corresponds to the dashed vertical line well inside the forward inertial range. These flux values have been normalized by their mean value, and the standard deviation is just 20% of the mean value, so the instantaneous flux values are dominated by their mean value and they are never negative. This allows fitting normal and gamma distributions to the data, and the latter seemingly yields a better fit. Collecting flux values at other wave numbers inside the inertial range gives virtually identical results, with the standard deviation ranging from 10% to 30%.

Turning to wave turbulence, a detailed study of the forward branch of a dual cascade was recently published in [8] (hereafter DB23). The underlying model was a member of the one-dimensional MMT model family developed in [9] and used as a testbed for wave turbulence theory ever since. The model is based on a complex wave function $\psi(x,t)$ that satisfies

$$i\psi_t = \mathcal{L}^\alpha \psi + |\psi|^2 \psi \tag{11}$$

in a periodic domain. This is the nonlinear Schrödinger equation with cubic nonlinearity and a modified linear term, which is defined on Fourier modes by $\mathcal{L}^\alpha \exp(ikx) = |k|^\alpha \exp(ikx)$. Four-wave resonances are possible if $0 < \alpha < 1$ and the simulations used $\alpha = 1/2$, for which the linear dispersion relation $\omega(k) = \sqrt{|k|}$ resembles that of deep-water surface waves. However, the precise value of α is not essential for the results, which has been validated using a comparison run with $\alpha = 3/4$ that did not change the outcome. [The full MMT model has an additional parameter that modifies the nonlinear terms, but here (11) is sufficient.] Standard white-noise forcing at $k = k_f$ and dissipation operators at k_- and k_+ were added, see DB23 for details. A forced–dissipative stationary state was reached and the power-law exponent of the spectral action density $n(k)$ in the forward inertial range was carefully measured. The prediction from the kinetic equation is $n \propto k^{-1}$, but the observed power law k^{-s} was invariably steeper, with a very slow convergence towards the k^{-1} slope (see left panel in Fig. 2). Crucially, the impact of the value of k_+ was felt across the entire inertial range and not just in the dissipation range. A reasonable empirical fit for s was [cf. (48) in DB23]

$$s \approx 1 + \frac{3}{2}\frac{\omega_f}{\omega_+}. \tag{12}$$

Achieving convergence is computationally demanding if $\omega = \sqrt{|k|}$, because then the frequency bandwidth is just half of the wave-number bandwidth. The right panel in Fig. 2 shows a histogram of (normalized) instantaneous wave energy flux values at $k = 400$ in the inertial range. In contrast to the situation in two-dimensional turbulence, there is now a much larger random component, the normalized standard deviation

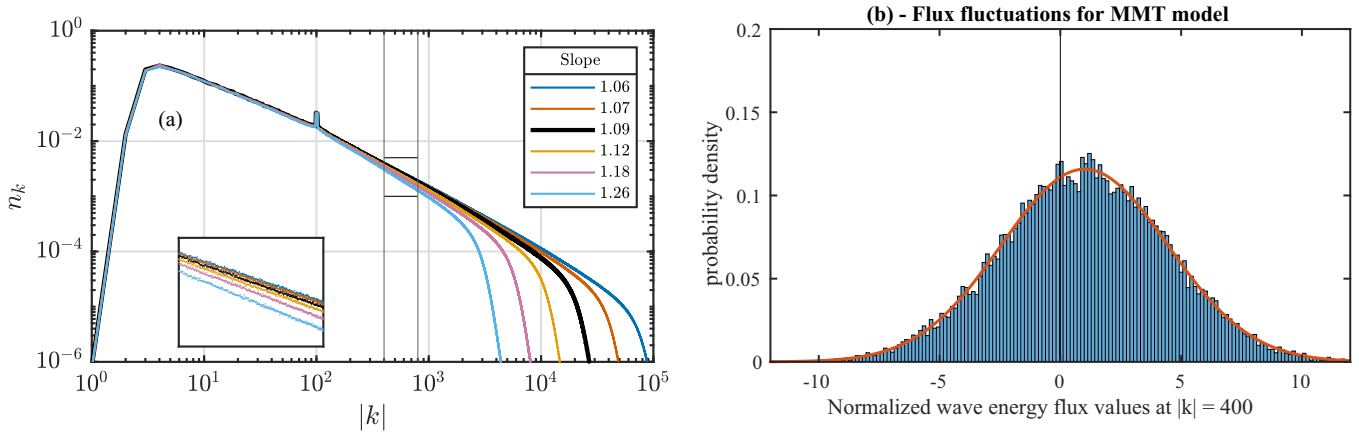

FIG. 2. Left: Action spectra and measured power laws in the forward inertial range for six MMT model simulations. The forcing is at $k_f = 100$, and the small-scale dissipation wave number k_+ doubled from run to run. A power law k^{-s} is fitted in the indicated observation window $k \in [400, 800]$ with results for s in the legend, showing very slow convergence to the ideal value $s = 1$. Right: Histogram of energy flux values (normalized to have unit mean) collected at $k = 400$ for the run with the second-smallest k_+. The standard deviation is 345% of the mean flux, almost 40% of observed values are negative, and there is a good fit with the normal distribution (solid line).

is a massive 340%, and almost 40% of observed values were *negative*, i.e., they had the opposite sign of the mean flux!

Comparing the two cases it is clear that the spectral slope is affected by the dissipation wave number much more strongly in the wave case, where it affects a large part of the inertial range. Second, the instantaneous wave energy flux values have a much stronger random component than the corresponding enstrophy fluxes, so much so that almost 40% of wave energy flux values were negative. This contrasts with 0% negative values in the hydrodynamic case. Finally, the flux fluctuations follow a normal distribution to a very good approximation in the wave case but decidedly not in the hydrodynamic case.

III. RANDOM WALK MODEL

We describe the model and study its predictive performance without attempting any rational justification for it. A discussion of whether the model can be so justified is deferred to Sec. IV. The derivation uses basic facts about Itô diffusions that can be found in textbooks such as [10,11].

A. Formulation of the model

Consider a lump or particle of wave action performing a continuous one-dimensional random walk in frequency space. Let $\Omega(t)$ be the frequency of the particle at time t, and let $\Omega(0) = \omega$ be its initial condition. The frequency domain $I = [\omega_-, \omega_+]$ is bounded, and the walk terminates when the particle hits either of the two boundary points. The evolution

$$\mathrm{d}\Omega(t) = \sqrt{2\gamma(\Omega)}\,\mathrm{d}W(t) \tag{13}$$

is a drift-free Itô diffusion with multiplicative noise. Here $\mathrm{d}W$ is the increment of a Wiener process, and the function $\gamma(\omega) > 0$ is arbitrary at this stage, except for the requirement that it is positive throughout the domain I.

The particle will exit I in finite time and the probability that it exits at the left boundary is a function of the initial condition $u(\omega)$ that satisfies the boundary-value problem

$$Lu = 0 \quad \text{with} \quad u(\omega_-) = 1 \quad \text{and} \quad u(\omega_+) = 0. \tag{14}$$

Here the operator

$$L = \gamma(\omega)\frac{\partial^2}{\partial\omega^2} \tag{15}$$

is the generator of the diffusion (13). The assumption $\gamma > 0$ reduces (14) to $u''(\omega) = 0$, and hence $u(\omega)$ is the straight line,

$$u(\omega) = \frac{\omega_+ - \omega}{\omega_+ - \omega_-}. \tag{16}$$

Conversely, the probability of exiting at the right boundary ω_+ is $1 - u(\omega)$. After identifying the forcing frequency ω_f with the initial condition $\Omega(0) = \omega$, we see that the exit probability for the lump of wave action in (16) is identical to the action flux rate predicted by Fjørtoft's dual-cascade argument in (10). Repeating the particle random walk many times will therefore result in a mean flux of wave action in agreement with (10), and the mean wave energy budget is then also satisfied. This demonstrates that it is possible to achieve the delicate dual-cascade flux balance in (10) by blind chance.

Persistent insertion of action lumps at ω_f at some fixed rate $R > 0$ per unit time leads to a forced–dissipative stationary state. The corresponding stationary action density $m(\omega)$ is a solution to the forced steady Fokker–Planck equation

$$0 = L^\dagger m + R\delta(\omega - \omega_f), \quad \text{where} \quad L^\dagger m = \frac{\partial^2}{\partial\omega^2}[\gamma(\omega)\, m] \tag{17}$$

is the adjoint of L, and $m(\omega_-) = m(\omega_+) = 0$. The overall magnitude of $m(\omega)$ is proportional to the injection rate R, but this does not affect the shape of $m(\omega)$. For transparency in the derivation we use $m(\omega_f) = 1$.

In the forward inertial range $\omega_f < \omega < \omega_+$, so (17) reduces to $L^\dagger m = 0$, which is solved by $\gamma m = a + b\omega$ with constants (a, b). Fitting to the boundary conditions yields

$$m(\omega) = \frac{\gamma(\omega_f)}{\gamma(\omega)}\,\frac{\omega_+ - \omega}{\omega_+ - \omega_f}. \tag{18}$$

To determine $\gamma(\omega)$ it is sufficient to postulate a theoretical power law for an ideal forward inertial range, i.e., an inertial

range with infinite frequency bandwidth ω_+/ω_f. This corresponds to the limit $\omega_+ \to \infty$ while keeping (ω, ω_f) constant. If the theoretical prediction is $m \propto \omega^{-y}$, then this implies $\gamma(\omega) = \omega^y$ up to an irrelevant factor and hence the final result

$$m(\omega) = \left(\frac{\omega_f}{\omega}\right)^y \frac{\omega_+ - \omega}{\omega_+ - \omega_f}, \quad \text{or} \quad m(\omega) = \frac{\omega_+ - \omega}{\omega^y} \tag{19}$$

up to a scaling factor. The frequency action density $m(\omega)$ is therefore a linear combination of *two* power laws, ω^{-y} and ω^{1-y}, and this is the main prediction of the model. A local power-law fit of (19) yields

$$-\frac{\partial \ln m}{\partial \ln \omega} = y + \frac{\omega}{\omega_+ - \omega}, \tag{20}$$

which is always steeper than the ideal slope y. The excess slope is proportional to ω/ω_+ for small $\omega/\omega_+ \ll 1$, which recovers the empirical finding (12) if the observation ratio ω/ω_f is kept constant. However, (12) was obtained for a wave-number action density $n(k)$, so (19) and (20) need to be adapted based on $n\mathrm{d}k = m\mathrm{d}\omega$.

This step depends on α, and assuming an even spectrum $n(k) = n(-k)$ it suffices to consider $k > 0$ so that $\omega = k^\alpha$. This yields

$$n(k) = \alpha k^{\alpha-1} m(k^\alpha) = \alpha k^{\alpha-1} \left(\frac{k_f}{k}\right)^{\alpha y} \frac{k_+^\alpha - k^\alpha}{k_+^\alpha - k_f^\alpha}. \tag{21}$$

Comparing (19) to (21) suggests that ω is a better variable than k. If $k_+ \to \infty$ then $n \propto k^{-z}$, with

$$z = 1 + \alpha(y - 1). \tag{22}$$

The counterpart of (20) is

$$-\frac{\partial \ln n}{\partial \ln k} = z + \alpha \frac{\omega}{\omega_+ - \omega}. \tag{23}$$

So the excess slope in k space is α times the excess slope in ω space. The theoretical slopes in the forward cascade of this MMT model are $z = y = 1$ for all values of α, and hence $n(k)$ is a linear combination of k^{-1} and $k^{\alpha-1}$. Notably, these consequences of the random walk model do not depend on fluctuations induced directly by the wave-forcing mechanism, in contrast with the situation explored in [12].

B. Comparison with direct numerical simulations

We consider again the left panel in Fig. 2, especially the legend, in which the slow convergence towards k^{-1} is quantified. To compare with the prediction from the random walk model

$$n(k) = \frac{k_+^{1/2} - k^{1/2}}{k} \tag{24}$$

(up to a factor) requires setting the effective value of k_+ for each simulation, which should be done in a very simple manner to avoid overfitting. The MMT model was simulated using a pseudospectral code with n Fourier modes so that the maximal wave number was $n/2$. The small-scale dissipation was tuned to restrict the excited wave-number band to $|k| < n/4$ for de-aliasing. This motivates the very simple choice

$$k_+ = \frac{n}{4} \tag{25}$$

for each run. (This agrees within 10% or so with more elaborate methods for choosing k_+ based on the actual dissipation spectral density computed by the model.) In the simulations n ranged from to 16 384 to 524 288, so the corresponding k_+ ranged from 4096 to 131 072.

First off, for small ω/ω_+ the random walk model (23) predicts an excess slope for $n(k)$ of size $\approx 0.5\omega/\omega_+$ and the empirical rule (12) had $1.5\omega_f/\omega_+$. To compare these two, note that the observation window $k \in [400, 800]$ corresponds to $\omega \in [20, 28]$, and with $\omega_f = 10$ the random walk prediction therefore ranges from $[1, 1.4]\omega_f/\omega_+$. This appears reasonably close to the empirical rule. But a much more precise comparison is given in the left panel of Fig. 3, which shows $n(k)$ for $k > k_f$ as predicted from (24) for the parameters of the direct numerical simulations. These look very similar to the bundle of MMT spectra in the left panel of Fig. 2. Moreover, the legend shows least-squares estimates for the slopes obtained by exactly the same least-squares method as in DB23. These are in very close agreement with the observed slopes in Fig. 2. Finally, the right panel in Fig. 3 shows in the same plot the observed and the modeled action spectra for the two runs with the lowest resolution, because for these runs the discrepancies from the ideal power law are strongest. The plots are offset by a decade for illustration purposes. Also plotted is the ideal slope k^{-1} as a thin straight line; all curves are pinned to coincide at $k = 169$, somewhat above $k_f = 100$. Clearly, the observed and the modeled spectra agree very well throughout the inertial range and even in the dissipation range. By contrast, the straight line for the ideal power law is clearly inaccurate in much of the inertial range and irrelevant in the dissipation range. Moreover, as suggested by a referee, it was checked that this is true also for the transient development of the spectrum: as the spectrum grows towards its forced–dissipative stationary state, its shape is already captured well by the random walk model.

In summary, in all cases the shape of the power spectrum is captured in detail by the random walk model after fitting only one parameter, the dissipation wave number k_+, by the straightforward Eq. (25).

C. Nonlinear diffusion model

Nonlinear diffusion models have a long history in both hydrodynamic and wave turbulence theory [e.g., Refs. 6,7, and references therein] and it is natural to compare their predictions to those of the random walk model. They are derived based on the assumption of strong locality of interactions in k space and combine that with further phenomenological assumptions about the inertial range. This results in a local conservation law for $E(k, t)$ in the form

$$\frac{\partial E}{\partial t} + \frac{\partial F}{\partial k} = 0 \tag{26}$$

in which the flux F is a function of $(k, E, dE/dk)$. Steady states of this equation form a one-parameter family of solutions (ignoring a second parameter trivially related to overall amplitude scaling). By construction, the ideal theoretical power law is a member of this family, but the additional parameter allows satisfying a finite boundary condition such as $E = 0$ at $k = k_+$. It is therefore natural to compare the

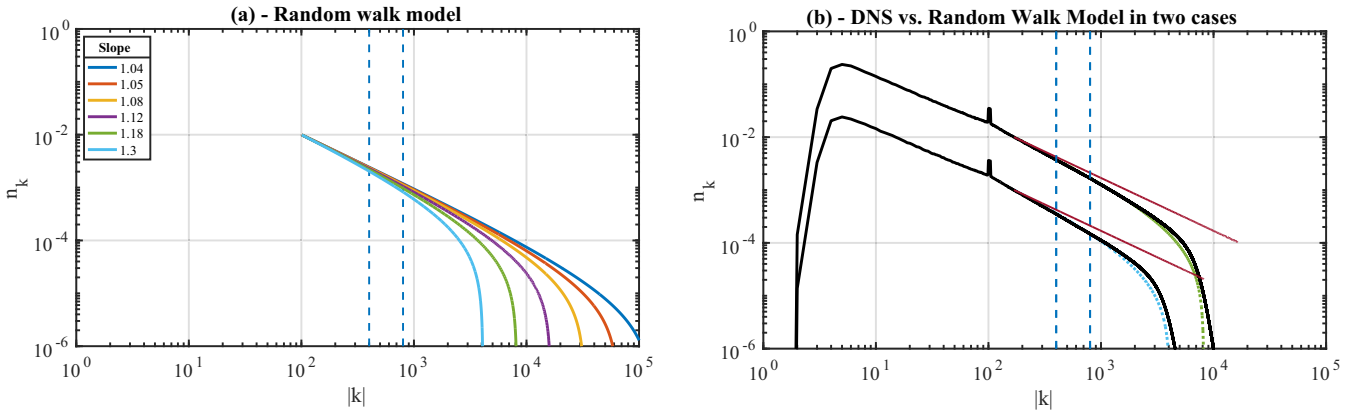

FIG. 3. Left panel: Shape of wave action spectra in the forward inertial range as predicted from the random walk model (18) for the six runs in Fig. 2. The dissipation wave number k_+ is chosen as in (25). The legend shows the predicted slopes using the same fitting method as in DB23, which are in very good agreement with those in Fig. 2. Right panel: Detailed comparison of simulated (solid lines) and predicted (dashed lines) spectra for the two runs with the lowest resolution. The spectra are offset by a decade for clarity. This shows a very good fit, whereas the ideal slope (indicated by the straight line) is significantly off.

predictions from the random walk model (which led to a linear diffusion equation) with the predictions of a nonlinear diffusion model for the MMT equation in the forward cascade. It is straightforward to derive such a model for the MMT system, though this does not seem to have been written down before.

The phenomenological assumptions for the flux F are threefold. First, $F = 0$ in a state of thermodynamic equilibrium. Second, $F = \text{const.}$ for the theoretical power law in the inertial range. And third, F should scale with E in a manner consistent with the relevant equations of motion. For the forward cascade in the MMT model this means $F = 0$ if E is constant (equipartition of energy), $F = \text{const.}$ if $E = \omega n = 1/\sqrt{k}$, and F should be proportional to E^3. The latter scaling is based on the kinetic equation for four-wave interactions and therefore differs from the scaling obtained directly from the MMT equation, which would be $F \propto E^2$; this reduction in flux efficiency for weak waves is a hallmark of wave turbulence theory. Hence

$$F = -k^{5/2}E^2\frac{\mathrm{d}E}{\mathrm{d}k}, \tag{27}$$

and the corresponding family of steady states is

$$E = (A - Bk^{-3/2})^{1/3} \tag{28}$$

with constants (A, B). Fitting to $E(k_+) = 0$ yields the action spectrum

$$\tilde{n}(k) = \frac{E}{\omega} = \frac{(k_+^{3/2} - k^{3/2})^{1/3}}{k} \tag{29}$$

up to a factor. This differs appreciably from the corresponding shape (24) based on the random walk model. Figure 4 shows plots of $\tilde{n}$ and the values of the associated slopes for the same six runs considered before. Clearly, the nonlinear diffusion model hews closely to the ideal slope k^{-1} for almost the entire inertial range and therefore captures none of the bending down of the action spectrum that was observed in the numerical simulations. This is confirmed by the measured power-law slopes, which are very different from those in the direct numerical simulations in Fig. 2. Overall, the nonlinear diffusion model delivers a poor fit to the wave turbulence

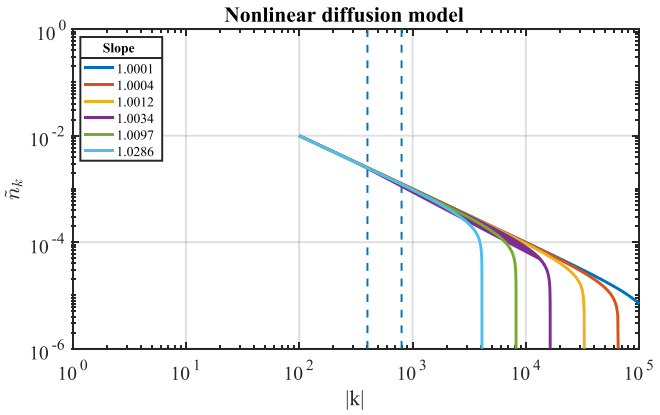

FIG. 4. Predicted shape of wave action spectra in the forward inertial range from the nonlinear diffusion model. Compared to Figs. 2 and 3, the action spectra is very close to the ideal k^{-1} throughout the inertial range.

TABLE I. Measured power-law slopes vs resolution for direct numerical simulation, random walk model, and nonlinear diffusion model.

Slope comparison summary			
k_+	DNS	RWM	NDM
4096	1.26	1.30	1.03
8192	1.18	1.18	1.01
16384	1.12	1.12	1.00
32768	1.09	1.08	1.00
65536	1.07	1.05	1.00
131072	1.06	1.04	1.00

spectra with finite bandwidth, and the opposite is true for the successful predictions of the random walk model. Of course, this finding in the present situation does not invalidate the productive use of nonlinear diffusion models in other wave turbulence problems. The results are summarized in Table I.

IV. DISCUSSION

The simple random walk model worked remarkably well for the forward cascade in this wave turbulence model, so it is natural to consider how to explore and test it in a wider range of settings and also whether the model could be derived from the underlying dynamics in a rational fashion.

The simplest extension within the current setup is to adapt it to the inverse part of the dual cascade based on the theoretical slope there, which differs from the $z = 1$ slope in the forward cascade. Numerically this regime can be explored by increasing k_+ while keeping k_f/k_+ constant. This is a straightforward process, albeit numerically demanding. DB23 did not consider the inverse cascade, so this requires new high-resolution simulations. The more significant extension is to work with a two-dimensional MMT system, which follows in a straightforward fashion from (11) by replacing $|k|$ with the magnitude of a two-dimensional wave-number vector. The two-dimensional MMT model covers basically the whole range of possible nonlinear Schrödinger equations with cubic nonlinearities, so this would be quite general. One could expect the flux fluctuations to be affected by the additional spatial dimension, which presumably reduces the amount of backscattered, negative flux in the inertial range. Conversely, it would be interesting to investigate a wave turbulence model based on three-wave interactions, which does not have a dual cascade, so it is an open question as to whether the flux fluctuations in such a model show the same level of apparent randomness.

Turning to the question of whether the model can be derived from the underlying equations, it is important to be aware of the shortcomings of the model as an illustration of the whole dynamics. First off, the model features strong conservation of action but only weak conservation of energy, i.e., action is conserved on every realization of the random walk but energy only in distribution, after averaging over many such realizations. This is, of course, different from the underlying dynamical system, which conserves both quantities strongly. A second issue is connected to this problem, namely, that a single lump of wave action seeded in the spectral domain manifestly does not behave in the manner envisaged here, if only for the conservation reason mentioned before. In other words, a single blob released into an otherwise empty spectrum would have to spread immediately if it were to move at all, as a well-known consequence of the dual conservation laws.

But this is less damning than it appears, because the particle in this model should really be interpreted in the spirit of a "test particle," a familiar concept in mean field theory and plasma physics [e.g., 13]. In this view there is a pre-existing broadband spectrum of waves and the weak test particle is released into the buffeting and push and pull due to all the modes in that broadband spectrum, but without feeding back onto them. Self-consistency is then established by making the resultant probability density of the test particle proportional to the spectral density of the broadband wave spectrum. This test particle concept also resolves the problem of weak conservation of wave energy, because now the test particle has only a tiny amount of action and energy compared to all the other modes. Therefore appreciable budget changes require many test particles, and this will result in accurate conservation of both action and energy by the law of large numbers. From this perspective the only necessary ingredient to the model is a prediction for the ideal cascade slope. Famously, this slope can be derived (at least formally) from the kinetic equation, but it is also well known that in many cases the same ideal cascade slope can be determined just from the assumption of self-similarity combined with scaling symmetries of the underlying equations (this is demonstrated for the MMT model in DB23). So the kinetic equation is not necessary and need not even be strictly valid for this approach to function.

We return to the fundamental question raised by the success of the random walk model in the present wave turbulence setting: What is the physical mechanism for the subtle balances in a dual cascade with a finite inertial range? It could be a complicated action-at-a-distance mechanism whereby the dissipation range k_+ affects the inertial range dynamics even of $k_f \ll k \ll k_+$. Or, it could be the inevitable outcome of blind chance.

ACKNOWLEDGMENTS

The hydrodynamic turbulence simulation and flux diagnostics were kindly produced by K. Shafer Smith. Ryan Dù produced the MMT simulations for DB23 and coauthored that paper. Sylvia Sun explored aspects of the random walk model during an undergraduate research experience at NYU. Helpful comments of anonymous referees were greatly appreciated. This work was supported by the Simons Collaboration on Wave Turbulence, and the numerical components were made possible thanks to New York University's Greene computing cluster facility. Additional financial support under Office of Naval Research (ONR) Grant No. N00014-19-1-2407 and National Science Foundation (NSF) Grant No. DMS-2108225 is gratefully acknowledged.

[1] U. Frisch, *Turbulence: The Legacy of A. N. Kolmogorov* (Cambridge University Press, Cambridge, 1995).

[2] R. Salmon, *Lectures on Geophysical Fluid Dynamics* (Oxford University Press, Oxford, UK, 1998).

[3] R. Fjørtoft, On the changes in the spectral distribution of kinetic energy for two-dimensional, nondivergent flow, Tellus A **5**, 225 (1953).

[4] V. E. Zakharov, V. S. L'vov, and G. Falkovich, *Kolmogorov Spectra of Turbulence I*, Springer Series in Nonlinear Dynamics (Springer, Berlin, Heidelberg, 1992).

[5] V. E. Zakharov, F. Dias, and A. Pushkarev, One-dimensional wave turbulence, Phys. Rep. **398**, 1 (2004).

[6] S. Nazarenko, *Wave Turbulence*, Lecture Notes in Physics Vol. 825 (Springer, Berlin, Heidelberg, 2011).
[7] S. Galtier, *Physics of Wave Turbulence* (Cambridge University Press, Cambridge, UK, 2022).
[8] R. S. Dù and O. Bühler, The impact of frequency bandwidth on a one-dimensional model for dispersive wave turbulence, J. Nonlinear Sci. **33**, 81 (2023).
[9] A. J. Majda, D. W. McLaughlin, and E. G. Tabak, A one-dimensional model for dispersive wave turbulence, J. Nonlinear Sci. **7**, 9 (1997).
[10] C. W. Gardiner *et al.*, *Handbook of Stochastic Methods* (Springer Berlin, 1985), Vol. 3.
[11] B. Oksendal, *Stochastic Differential Equations: An Introduction with Applications* (Springer Science & Business Media, New York, 2013).
[12] E. Falcon, S. Aumaître, C. Falcón, C. Laroche, and S. Fauve, Fluctuations of energy flux in wave turbulence, Phys. Rev. Lett. **100**, 064503 (2008).
[13] P. H. Diamond, S.-I. Itoh, and K. Itoh, *Modern Plasma Physics: Volume 1, Physical Kinetics of Turbulent Plasmas* (Cambridge University Press, Cambridge, UK, 2010).